PHYSICAL REVIEW B **74**, 125416 (2006)

Optical properties of pentacene thin films and single crystals

Daniel Faltermeier, Bruno Gompf,* Martin Dressel, Ashutosh K. Tripathi, and Jens Pflaum
Physikalisches Institut, Universität Stuttgart, Pfaffenwaldring 57, D-70550 Stuttgart, Germany

(Received 24 March 2006; revised manuscript received 26 May 2006; published 15 September 2006)

The optical properties of pentacene single crystals and thin films are systematically investigated by variable angle spectroscopic ellipsometry. In combination with x-ray diffraction and atomic force microscopy the method allows us to distinguish between the complex optical constants (n and k) of the different polymorphs formed in thin films during the growth process. On the biaxial anisotropic single crystal it is possible to determine the optical constants along the respective crystallographic orientations. Temperature-dependent measurements in the range from $T=5$ K to 350 K confirm the assignment of the optical spectra. The results are in good agreement with *ab initio* calculations of the optical properties of solid pentacene by Tiago *et al.* [Phys. Rev. B. **67**, 115212 (2003)].

DOI: 10.1103/PhysRevB.74.125416 PACS number(s): 68.55.−a, 71.35.Cc, 72.80.Le, 78.20.−e

I. INTRODUCTION

Pentacene is one of the most promising organic materials for future applications, e.g., in low-cost organic field-effect transistors (OFETs). For many years its electronic and transport properties have been widely studied and by now, thin film transistors made of highly ordered films exhibit mobilities around 1 $\mathrm{cm}^2/\mathrm{V\,s}$.[1,2] Despite these efforts the correlation between film morphology and its function is still not well understood. The transport and the optical properties of organic thin films are determined by grain boundaries, traps, and imperfections of the film morphology. Depending on the growth conditions, in the case of pentacene up to four different polymorphs can be identified by x-ray diffraction, and all of them have different electronic and optical properties,[3–5] but not all are thermodynamically stable. To get access to the intrinsic properties of these materials, for example, the material-dependent mobility for electrons and holes or the role of impurities or gap states, additional investigations on single crystals are essential.[6–8] Furthermore, a comparison to theoretical predictions is only possible for measurements on well-defined systems. There exist now an increasing number of band-structure calculations[9–11] for organic semiconductors which make predictions on the intrinsic mobility or the optical band gap.[9,12,13] Although the influence of different polymorphs on the mobility is a heavily discussed problem, the consequences for the optical properties[14,15] are not well studied. For example, the complete anisotropic complex dielectric function is so far determined only for a very small number of the widely discussed organic semiconductors (e.g., for PTCDA).[16,17]

Pentacene crystallizes in a triclinic lattice. The optical behavior of absorbing biaxial crystals with symmetry lower than orthorhombic is quite complex. The reason is because, in general, in these materials the principal axes of the two index ellipsoids, one for **n** and one for **k**, are neither parallel to each other nor to the crystallographic axes, and their directions rotate with energy.[18] From these ellipsoids it is still possible to get n and k in any direction, but their relation is more complex than the standard Kramers-Kronig relation.

Indeed generalized spectroscopic ellipsometry allows us to determine the optical properties of inhomogeneous and/or anisotropic media in all details and with very high accuracy, but the necessary formalism to characterize absorbing low-symmetry materials has not been worked out so far.

In this paper we present an ellipsometric study on pentacene single crystals and thin films, compare the results with band-structure calculations, and discuss the problems connected to the low-crystal symmetry.

II. EXPERIMENTS

To minimize impurities, pentacene (purchased by Fluka) is purified twice by gradient sublimation before being used as starting material. The films were prepared in UHV at a base pressure of about 7×10^{-7} Pa from a graphite effusion cell. The evaporation rate was about 3 Å/s; it was controlled by a quartz microbalance located next to the sample. As a substrate we used cleaned Si(100) wafers which were thermally oxidized with 200 nm of $\mathrm{SiO_2}$. This range of oxide thickness was necessary to reliably perform OFET measurements. Using top contact geometry, we achieved mobilities of approximately 0.1 $\mathrm{cm}^2/\mathrm{V\,s}$. The OFET results will be published elsewhere. After preparation, the film morphology was characterized *ex situ* at room temperature by x-ray diffraction and atomic force microscopy (AFM).

For the growth of pentacene single crystals, we applied the gas-flow reactor method, which is commonly used for organic compounds that can only be sublimated.[19] Similar to the thin film growth, two-times gradient-sublimated pentacene was used also for the crystal preparation. Over a total period of 50 h the crystals were grown in a steep temperature gradient under a constant stream (50 cm^3/s) of forming gas (approximately 4% $\mathrm{H_2}$ contents). The sublimation temperature under these conditions amounts to about 573 K; the starting material, as well as the resulting pentacene single crystals, were handled under yellow light to minimize further photo-oxidation processes on the sample surfaces.

The x-ray studies were performed in the Bragg-Brentano geometry, using Cu Kα_1 radiation at a wavelength of 1.5418 Å. According to this scattering geometry, the momentum transfer is normal to the surface of the sample. Figure 1 shows the result for films prepared at three different substrate temperatures. The lattice parameters of two different polymorphs can be clearly distinguished; both show a strong preferential alignment of the (001) plane parallel to the sub-

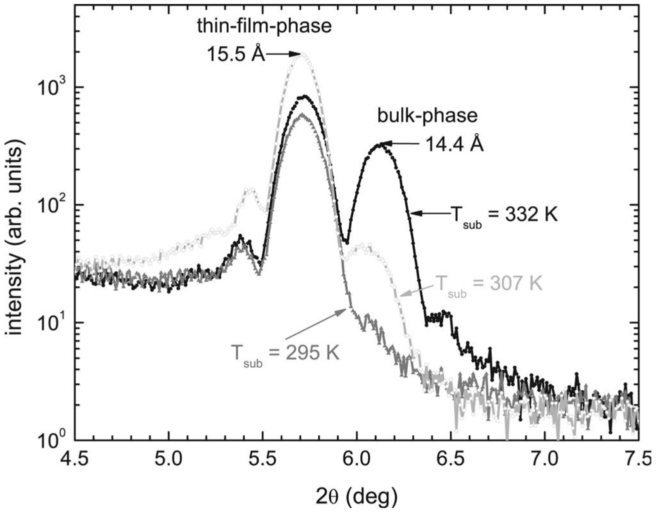

FIG. 1. X-ray diffraction data from thin pentacene films prepared at different substrate temperatures. With increasing substrate temperature the amount of the so-called bulk phase in the film increases.

strate surface. Additional rocking curves, not shown here, reveal a rocking width below 0.15°. In agreement with literature[3] we found at reduced substrate temperatures and low coverages, the so-called "thin-film phase" characterized by a (001) lattice spacing of 15.5 Å. At higher substrate temperatures additionally the so-called "bulk phase" starts to evolve with a (001) spacing of 14.4 Å. It has to be stressed that both of these polymorphs differ from the single-crystal phase where the (001) spacing is only 14.1 Å.[5,20] The growth of a second phase at higher substrate temperatures is also indicated by atomic force microscopy (AFM) on these films (Fig. 2). At low substrate temperatures where a nearly pure thin film phase can be grown (see Fig. 1) the films are very flat, whereas at elevated substrate temperatures additionally large three-dimensional (3D) islands are formed.[21] The combination of x-ray and AFM investigations gives a consistent model of the film morphology at the different substrate temperatures.

For the optical characterization a Woollam vertical VASE equipped with a Berek compensator was utilized. The measurements were performed in the energy range between 0.5 and 4.0 eV with a resolution of 10 meV under multiple angles of incidence between 55°–75° and 25°–80° for the films and the single crystal, respectively. For temperature-dependent measurements the ellipsometer was equipped with a He-flow UHV cryostat. In the cryostat a base pressure below 10^{-7} Pa is required to avoid surface contamination during the measurements at low temperatures. Due to the 70° angle of the two cryostat windows, at low temperatures only measurements in a range between a 65°–75° angle of incidence are possible. To get access to the complex optical anisotropy, the data were analyzed with the program WVASE 32, which is based on the concept of generalized ellipsometry. For details, see Schubert and collaborators.[22,23] The program can handle biaxial crystals where the three principal axes for n and k are all orthogonal and parallel to each other. For each axis the dielectric function is parametrized by model dielectric functions. As result of the fit to the ellipsometric angles, the program displays six spectra (n and k along the three principal axes x, y, z) and three Euler angles Φ, Θ, Ψ, which give the orientation with respect to the laboratory coordinate system spanned by the plane of incidence, the normal to that plane, and the normal to the sample surface.

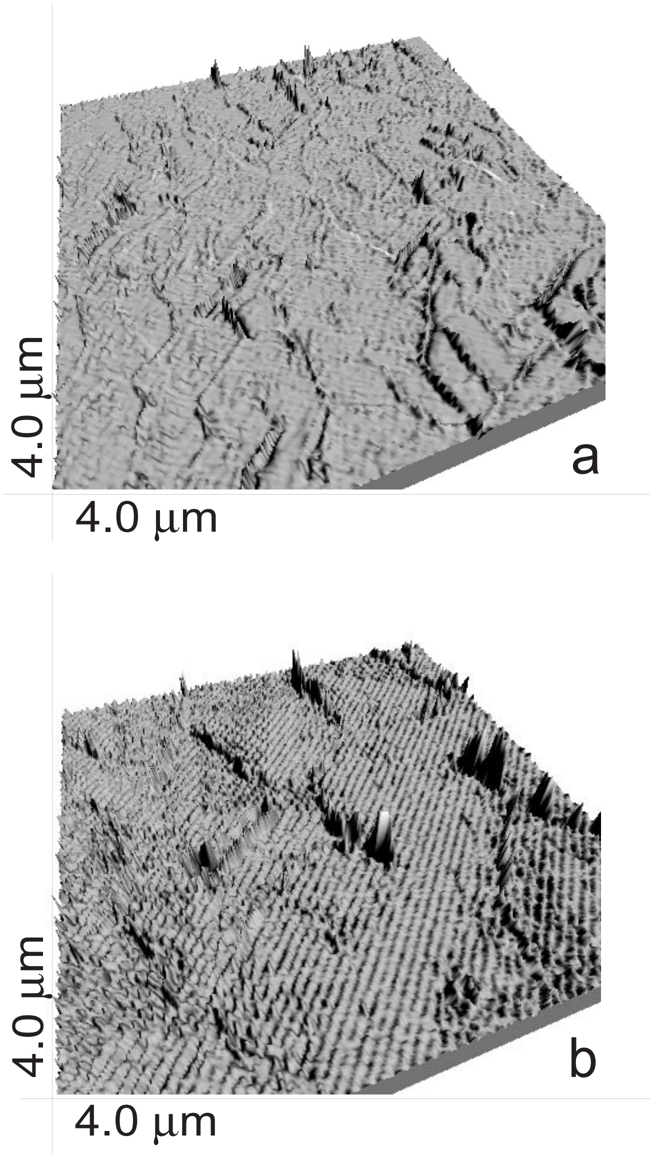

FIG. 2. AFM images of two pentacene films grown at (a) $T = 295$ K and (b) 331 K, respectively. (a) At low substrate temperatures the flat thin-film phase is built. (b) At higher substrate temperatures three-dimensional islands (bulk phase) are formed leading to a very rough surface.

III. RESULTS

Prior to the film preparation the bare Si/SiO$_2$ substrates were measured and the obtained parameters were later put into the further fit procedures. The ellipsometric thin film spectra could be modeled by assuming optical isotropy for

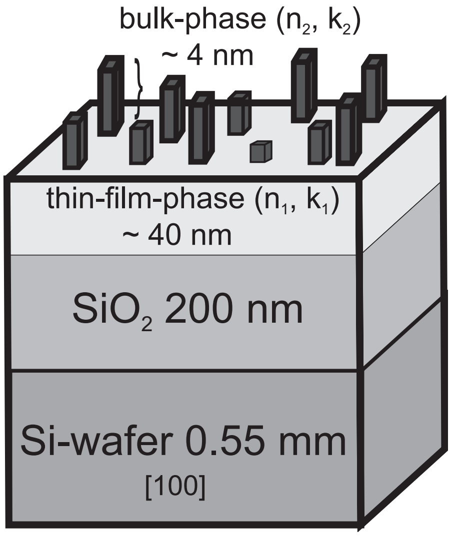

FIG. 3. Scheme of the layer structure used for the ellipsometric analysis.

each layer and the following layer structure: Si-wafer/ SiO_2/smooth pentacene layer 1 with the optical constants n_1 and k_1/rough pentacene layer 2 with the optical constants n_2 and k_2. In Fig. 3 a scheme of the assumed layer stack is depicted. In this model, layer 1 is described by five Gaussian oscillators [Eq. (1)] and layer 2 by an effective medium layer with 27% voids and three Gaussian oscillators. For none of the pentacene films, prepared at different sample temperatures, we found a conversion from p to s polarization, hence the ellipsometric data explicitly exclude an in-plane anisotropy in good agreement with recent ellipsometric results in the infrared.[24]

The n and k values obtained in this way for films prepared at different sample temperatures are plotted in Figs. 4 and 5 as a function of frequency. Layer 1 is identified as the thin film phase, layer 2 as the bulk phase. It was not possible to obtain reasonable fits under the assumption of only one pentacene layer. The optical response of the two polymorphs is clearly different, whereas the differences between several substrate temperatures within one polymorph is very small. Each crystallographic phase has its distinct optical signature independent of the thickness.

For the characterization of the single-crystal sample, the spectroscopic ellipsometer was equipped with a microfocus, which allows spot sizes down to 200 μm, a prerequisite to perform measurements on the small plane (001) terraces under various angles of incidence. The crystal dimensions were $6 \times 0.8 \times 0.06$ mm^3 with the long axis roughly parallel to the a direction. The samples were mounted inside the ellipsometer with their a direction parallel to the plane of incidence. Due to the small width and the not completely planar surface, it was not possible to perform reliable measurements at different in-plane azimuth angles.

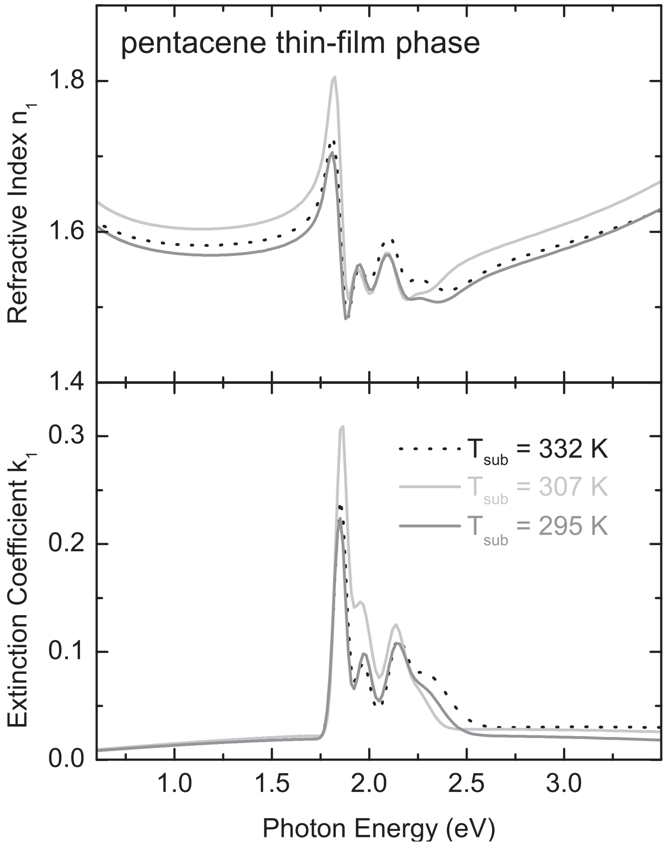

FIG. 4. Real and imaginary parts of the refractive index, n_1 and k_1, of the pentacene thin-film phase. The optical properties vary only slightly with the substrate temperature.

The data were fitted to the measured ellipsometric angles with the above-mentioned assumptions. The principal axes x, y, z for **n** and **k** are orthogonal, and their directions are energy independent. In pentacene the unit cell angles β (87.7°) and γ (84.7°) are nearly 90°, only α (76°) deviates a little bit more. On the one hand, the assumption of dispersion-free principal axes in triclinic systems is only valid for low-absorbing materials. On the other hand, the parametrization with model dielectric functions along orthogonal dispersion-free optical axes conserve the Kramers-Kronig consistency and therefore allows us comparison with calculated excitations. For the fit two Gaussian oscillators for the electric field vector $E \| y$ and $E \| z$ and three for the polarization $E \| x$ were used:

$$\epsilon_{n2} = A_n \exp - \left[\frac{E - E_n}{\Delta_n} \right]^2 + A_n \exp - \left[\frac{E + E_n}{\Delta_n} \right]^2 . \qquad (1)$$

Furthermore, a small roughness on top of the crystal was assumed. No indication for an additional oxidation layer on the crystal surface was found.

The result of the analysis is shown in Fig. 6 and Table I. The obtained Euler angles, e.g., the orientation of x, y, z in respect to the laboratory coordinate system is the following: the principal z axis is tilted against the surface normal in the plane-of-incidence by about −10° so that it is nearly parallel to the long axis of the molecules in the crystal. Thereby the x-y plane is tilted against the a-b plane by the same amount. For the x and y directions the oscillators could be fitted to the measured Ψ and Δ spectra with mean-square errors around 2. This is a remarkably good agreement, keeping in mind that the analysis ignores the triclinic-lattice structure. Only the z

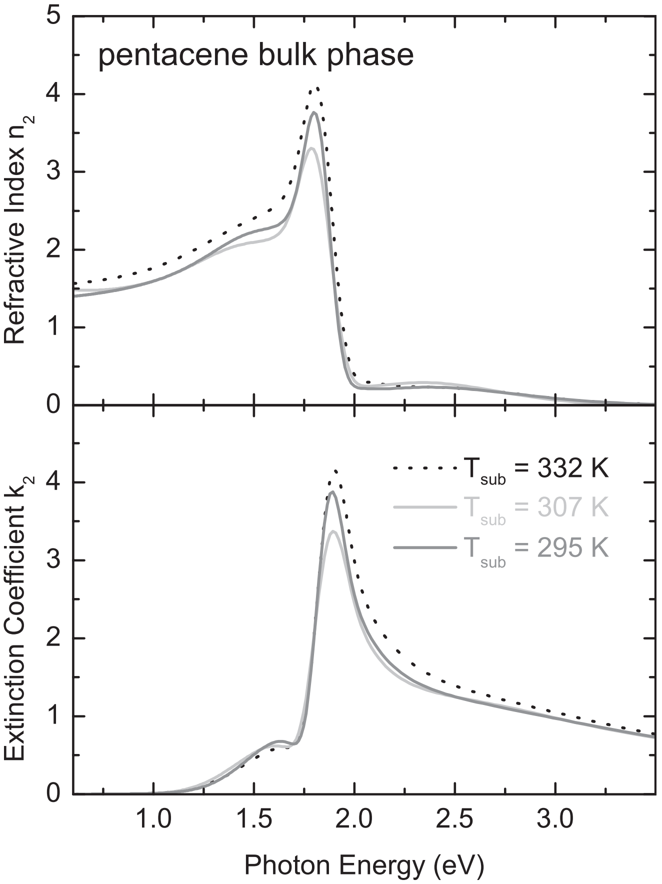

FIG. 5. n_2 and k_2 of the pentacene bulk phase. The overall optical behavior is clearly different from the thin-film phase.

direction could not be fitted with reasonable values. Particularly the peak amplitudes were much too high. Nevertheless the peak energies were in good agreement with theory (see below). The result for the z direction is, therefore, not included in Fig. 6 but for information, the corresponding oscillator positions are listed in Table I.

IV. DISCUSSION

In an isolated pentacene molecule the highest occupied molecular orbital (HOMO) has B_{1g} symmetry and the lowest unoccupied molecular orbital (LUMO) B_{2u} symmetry. Due to the intermolecular interaction and the existence of two nonequivalent molecules in the unit cell, two pairs of bands arise in the crystal, each with a finite bandwidth. In the molecule the π to π^* transition is polarized along the short molecular axis. Since the molecules are oriented with their long axis almost along the c direction of the crystal and the corresponding overlap between the molecules is rather weak, the optical activity is weak along the z and c direction, respectively. Equivalent arguments explain the strong optical response for polarization along the $x(a)$ axis and a medium response along the $y(b)$ direction. Additionally in organic semiconductors the optical band gap is masked by strong exciton absorption peaks located a few tens of meV below the conduction band.

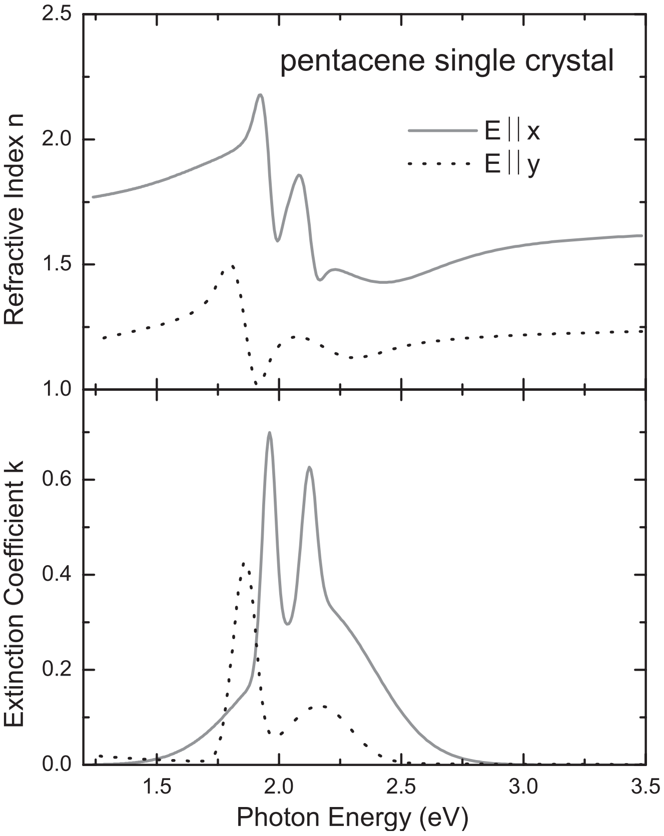

FIG. 6. Optical constants of pentacene single crystals parallel to the x and y principal axes as obtained by generalized spectroscopic ellipsometry.

For a more quantitative analysis we compare our results with *ab initio* calculations of the optical properties of different pentacene polymorphs by Tiago *et al.*[9] In this work the quasiparticle energies were calculated within the *GW* approximation and the electron-hole excitations by solving the Bethe-Salpeter equation. For the single crystal structure (labeled Structure *V* by Tiago *et al.*) they found a band gap E_g of 1.9 eV with a strong anisotropic bandwidth W. Here W is rather small in the c direction, but increases by one order of

TABLE I. The optical behavior of pentacene single crystals can be described by two Gaussian oscillators for the polarization $E\|y$ and $E\|z$ and three for $E\|x$.

	E_n (eV)	A_n	Δ_n
$E\|x$	1.95	1.84	0.06
	2.12	1.06	0.07
	2.12	1.05	0.58
$E\|y$	1.85	1.08	0.11
	2.16	0.28	0.30
$E\|z$	1.81	36.28[a]	0.09
	2.07	5.07[a]	0.59

[a] It was not possible to get reasonable values for the out-of-plane ($E\|z$) oscillator strength.

magnitude when going along the *a* or *b* axes with values of up to 0.67 eV. The lowest-energy exciton, a charge-transfer exciton, in their work is at 1.7 eV and the Davydov splitting is estimated to be 0.13 eV. Except for the fact that the theory yields an energy scale redshifted by about 0.1 eV compared to our results, the agreement between theory and experiment is remarkable, although the principal axes are slightly tilted against the crystallographic axes. In our measurements the lowest-lying exciton polarized along the $y(b)$ direction is at 1.85 eV, the perpendicular polarized Davydov component along $x(a)$ direction is at 1.95 eV. The measured interband absorption of 0.58 eV along the $x(a)$ axis is about twice as broad, compared to the $y(b)$ direction, which also perfectly agrees with the theoretical prediction. Even the ratio of the ϵ_2 values for the $x(a)$ and $y(b)$ axes is about 2, both in theory and experiment. Only the absolute values of ϵ_2 disagree by about a factor of 2. We found a maximum ϵ_2 value of 2.7, whereas Tiago *et al.*[9] gets an $\epsilon_2 \approx 5$. There are two possible explanations for this discrepancy. The deviation of the principal axes from the crystallographic axes can lead to an underestimation of the experimental values and/or the neglected electron-phonon coupling in the calculations will lead to an overestimation of the optical constants at room temperature, as demonstrated by the temperature-dependent measurements in Fig. 7. As can be seen from Fig. 6 and Table I there is a second sharp peak at 2.12 eV in the k spectrum along the *x* direction. Tiago *et al.* also found a small second peak along the a direction, but they neglect electron-phonon interactions in their calculations. Therefore, a vibronic nature of this peak cannot be generally excluded.

Except for the missing in-plane polarization in the thin-film phase (Fig. 4), the overall behavior of the film spectra is similar to that of the single crystal. Also the Davydov splitting can be observed at nearly the same energy. The interband absorption, as well as the overall extinction, is smaller, as expected for a less-dense phase. In the so-called bulk phase the situation is more complex. Here the shape of the small, but tall, crystallites on top of the thin-film phase might cause an overestimation of the optical constants along the *z* direction in the ellipsometric data analysis, thus dominating the whole spectrum. As for the *z* direction in the single crystal, the calculated absolute values for n_2 and k_2 in the thin films are much too high. But in contrast to a well-ordered system, where the optical constants can be separated along the different principal axes, the whole spectrum of a disordered layer appears with unrealistic high optical constants. Apart from the absolute values of the optical constants, the bulk-phase spectrum nevertheless resembles the calculated behavior for $\epsilon_2(\omega)$ of the solution phase considered in the theoretical work by Tiago *et al.*[9] (labeled as Structure *S*). Our generalized spectroscopic ellipsometry experiments clearly confirm that the optical properties depend very critically on the particular crystal structure and that it is possible to separate individual optical constants of each polymorph present in a thin film.

To support our optical assignment, we additionally carried out temperature-dependent ellipsometric measurements. To that end a thin pentacene film was prepared which consisted almost exclusively of the thin-film phase. Due to the large working distance in the cryostat, the microfocus cannot be utilized and, therefore, measurements on the small single crystals were not possible. Figure 7 shows the result in the energy and temperature range between 1.5 to 2.5 eV and $T = 5$ to 350 K, respectively. With decreasing temperature the optical gap is reduced and the Davydov splitting is enlarged from 0.1 eV at $T=300$ K up to 0.125 eV at $T=5$ K, leading to a redshift of peak *a* and a blueshift of peak *b*. This behavior is mainly due to the large thermal contraction typical for van der Waals–bonded organic crystals which leads to an enhanced orbital overlap at low temperatures. While these two peaks behave as expected, peak *c* did not shift at all. This would be an atypical behavior for a vibronic mode. Therefore this peak is presumably also an exciton, as predicted by Tiago *et al.*

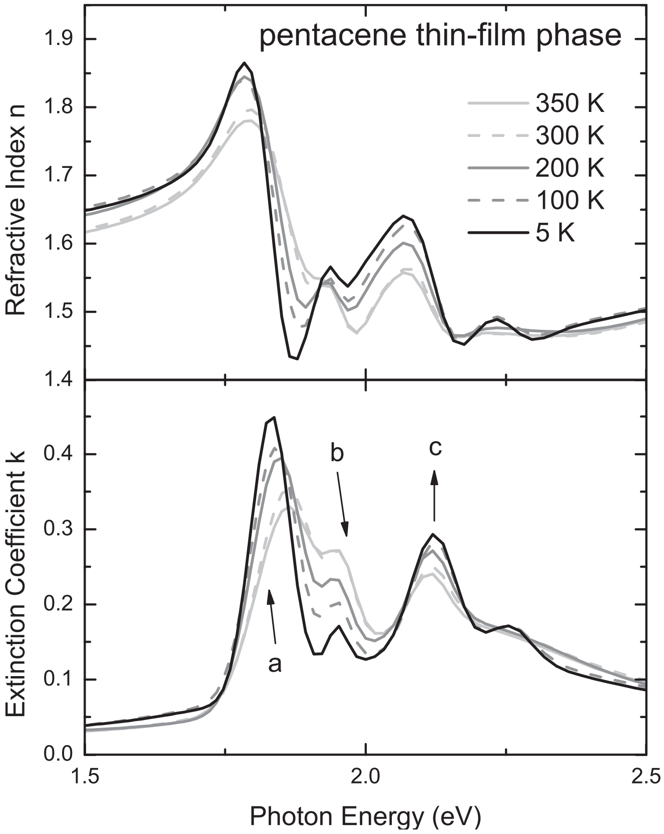

FIG. 7. Temperature-dependent ellipsometric measurement on a film containing nearly exclusively the thin-film phase. As expected for a molecular crystal, the optical band gap decreases and the Davydov splitting of around 0.1 eV at $T=300$ K increases with decreasing temperature up to 0.125 eV.

V. CONCLUSION

In a systematic study the optical properties of pentacene single crystals and thin films have been estimated by means of spectroscopic ellipsometry. In combination with x-ray diffraction and AFM, this method allows a distinction between the complex optical constants (*n* and *k*) of the different polymorphs generated in thin films during the growth process. Each crystallographic phase can be characterized by its specific optical behavior. On pentacene single crystals we were able to determine the biaxial anisotropic complex optical constants along the three principal axes in the framework of generalized spectroscopic ellipsometry. Although the principal axes deviate from the crystallographic axes, the results are in good agreement with *ab initio* calculations of the excitation spectrum by Tiago *et al.*[9]

ACKNOWLEDGMENTS

We acknowledge support by the Deutsche Forschungsgemeinschaft (DFG) under Grants Nos. GO 642/6 and PF 385/2. We also thank Steffen Hergert from the Institut für Systemtheorie und Bildschirmtechnik at the University of Stuttgart for experimental assistance by the film preparation.

---

*Electronic address: gompf@pi1.physik.uni-stuttgart.de

[1] C. D. Dimitrakopoulos and D. J. Mascaro, IBM J. Res. Dev. **45**, 11 (2001).

[2] O. D. Jurchescu, J. Baas, and T. T. M. Palstra, Appl. Phys. Lett. **84**, 3061 (2004).

[3] C. C. Mattheus, A. B. Dros, J. Baas, G. T. Oostergetel, A. Meetsma, J. L. de Boer, and T. T. M. Palstra, Synth. Met. **138**, 475 (2003).

[4] I. P. M. Bouchoms, W. A. Schoonveld, J. Vrijmoeth, and T. M. Klapwijk, Synth. Met. **104**, 175 (1999).

[5] T. Siegrist, C. Kloc, J. H. Schon, B. Batlogg, R. C. Haddon, S. Berg, and G. A. Thomas, Angew. Chem., Int. Ed. **40**, 1732 (2001).

[6] A. Vollmer, O. D. Jurchescu, I. Arfaoui, I. Salzmann, T. T. M. Palstra, P. Rudolf, J. Niemax, J. Pflaum, J. P. Rabe, and N. Koch, Eur. Phys. J. E **17**, 339 (2005).

[7] R. He, X. Chi, A. Pinczuk, D. V. Lang, and A. P. Ramirez, Appl. Phys. Lett. **87**, 211117 (2005).

[8] D. V. Lang, X. Chi, T. Siegrist, A. M. Sergent, and A. P. Ramirez, Phys. Rev. Lett. **93**, 086802 (2004).

[9] M. L. Tiago, J. E. Northrup, and S. G. Louie, Phys. Rev. B **67**, 115212 (2003).

[10] K. Doi, K. Yoshida, H. Nakano, A. Tachibana, T. Tanabe, Y. Kojima, and K. Okazaki, J. Appl. Phys. **98**, 113709 (2005).

[11] J. E. Northrup, M. L. Tiago, and S. G. Louie, Phys. Rev. B **66**, 121404 (2002).

[12] A. Troisi and G. Orlandi, J. Phys. Chem. B **109**, 1849 (2005).

[13] R. C. Haddon, X. Chi, M. E. Itkis, J. E. Anthony, D. L. Eaton, T. Siegrist, C. C. Mattheus, and T. T. M. Palstra, J. Phys. Chem. B **106**, 8288 (2002).

[14] S. P. Park, S. S. Kim, J. H. Kim, C. N. Whang, and S. Im, Appl. Phys. Lett. **80**, 2872 (2002).

[15] T. Aoki-Matsumoto, K. Furuta, T. Yamada, H. Moriya, K. Mizuno, and A. H. Matsui, Int. J. Mod. Phys. B **15**, 3753 (2001).

[16] M. I. Alonso, M. Garriga, N. Karl, J. O. Osso, and F. Schreiber, Org. Electron. **3**, 23 (2002).

[17] M. I. Alonso and M. Garriga, Thin Solid Films **455-56**, 124 (2004).

[18] M. Born and E. Wolf, *Principles of Optics* (Cambridge University Press, London, 1999).

[19] R. W. I. de Boer, M. E. Gershenson, A. F. Morpurgo, and V. Podzorov, Phys. Status Solidi A **201**, 1302 (2004).

[20] C. C. Mattheus, A. B. Dros, J. Baas, A. Meetsma, J. L. de Boer, and T. T. M. Palstra, Acta Crystallogr., Sect. C: Cryst. Struct. Commun. **57**, 939 (2001).

[21] T. Jentzsch, H. J. Juepner, K. W. Brzezinka, and A. Lau, Thin Solid Films **315**, 273 (1998).

[22] M. Schubert, B. Rheinlander, E. Franke, H. Neumann, T. E. Tiwald, J. A. Woollam, J. Hahn, and F. Richter, Phys. Rev. B **56**, 13306 (1997).

[23] M. Schubert, Thin Solid Films **313**, 323 (1998).

[24] M. Schubert, C. Bundesmann, G. Jacopic, H. Maresch, and H. Arwin, Appl. Phys. Lett. **84**, 200 (2004).